

Spectroscopic, Molar Conductance and Biocidal Studies of Pt(IV), Au(III) and Pd(II) Chelates of Nitrogen and Oxygen Containing Schiff Base Derived from 4-Amino Antipyrine and 2-Furaldehyde

Foziah A. Al-Saif

Department of Chemistry, Faculty of Science, Princess Nora Bint Abdul Rahman University, Riyadh, Kingdom Saudi Arabia

E-mail: foziah2013@yahoo.com

Received: 7 May 2013 / Accepted: 8 July 2013 / Published: 1 August 2013

Pt(IV), Au(III) and Pd(II) complexes of Schiff bases derived from 2-furaldehyde and 4-amino antipyrine (4APF) are reported and characterized based on elemental analyses, IR ¹H-NMR, electronic spectra, molar conductance, and thermal analysis (TG/DTG). The complexes are found to have the formulas [Pt(4APF)Cl]Cl₃, [Pd(4APF)]Cl₂ and [Au(4APF)(Cl)₂]Cl. The molar conductance data reveal that all the metal chelates of the 4APF ligand are electrolytes with different numbers of ionizable chloride ions. IR spectra show that 4APF is coordinated to the metal ions in a bi-dentate situation, with ON donor sites of azomethine-N and furan-O, whereas the Pt(IV) metal ions is coordinated to the 4APF in a tri-dentate situation with ONO donor sites of azomethine-N, furan-O, and carbonyl-O. The thermal behavior of these chelates shows that the hydrated complexes lose water molecules of hydration in the first step and is followed by decomposition of the anions and ligand moieties in the respective steps. The synthesized ligands, in comparison to their metal complexes, were also screened for their antibacterial activity against bacterial species as well as fungi. The activity data show the metal complexes to be more potent antimicrobial than the parent Schiff base ligand.

Keywords: 4-Amino antipyrine, 2-furaldehyde, noble metal, IR, ¹H-NMR, thermal analysis, biological and anticancer activities.

1. INTRODUCTION

Due to the fact that antipyrine derivatives are stable, useful intermediates, for the synthesis of other substrates and precursors of substances with biological activities, interest in studying these compounds has been continued [1-5]. In bio-functional compound aspects, broad properties of

antipyrene nucleus such as: antitumor [6-8], antimicrobial [9-11], antiviral [12, 13], anticancer [4, 14], analgesic drugs [15] and optoelectronic material aspects [16, 17]. Azomethine group (-C=N-) is the effective group of the compounds that know Schiff bases, which are usually synthesized by the condensation of primary amines and active carbonyl groups. Schiff bases represent important class of compounds in medical and pharmaceutical field [18] and it has many applications in important biological field [19], further move it act as corrosion inhibitors [20], catalysts [21-23]. Schiff base transition metal complexes are one of the most adjustable and totally studied systems [24, 25], these complexes have applications in clinical [26] and analytical fields [27]. Some of these complexes play important role in biological oxygen carrier systems [28]. The synthesis and characterization of these compounds have been described by small number of papers [29-35], Rosa and others [36] presented the synthesis of Cu(II) complexes derived from Schiff base ligand obtained by condensation of 4-aminoantipyrene with 2-hydroxybenzaldehyde and terephthalic aldehyde, then they continued in their studies [37] by use other salt of Cu(II) as well as other complexes of V(IV) and Ni(II), then they synthesized and characterized [38] new complexes of Cu(II) with Schiff base obtained by the condensation of 4-aminoantipyrene with 2-hydroxy-4-methoxy-benzaldehyde. Two antipyrene derivatives are structurally similar Schiff bases derived from the condensation of 2,3-dichlorobenzaldehyde or 2,5-dichloro-benzaldehyde with 4-aminoantipyrene in metal solution the compounds were characterized [39] by spectroscopic techniques. Broad spectra of bioactive 4-amino-antipyrene derivatives and their metal complexes have been investigated and diversities of bioactivities. Such as analgesic [39, 40], anti-inflammatory, antimicrobial [41, 42] and anticancer activity [43] have been reported.

Upon the great importance of 4-aminoantipyrene nucleus, this paper aimed to synthesized and characterization of new Au(III), Pt(IV) and Pd(II) Schiff base complexes derived from 4-aminoantipyrene with furaldehyde. There are many spectroscopic tools utilized to characterized the synthesis complexes elemental analysis, molar conductivity, (NMR, infrared and UV-Vis) spectra, thermal analyses (TG/DTG), X-ray power diffraction (XRD) as well as scanning electron microscopy (SEM).

2. EXPERIMENTAL

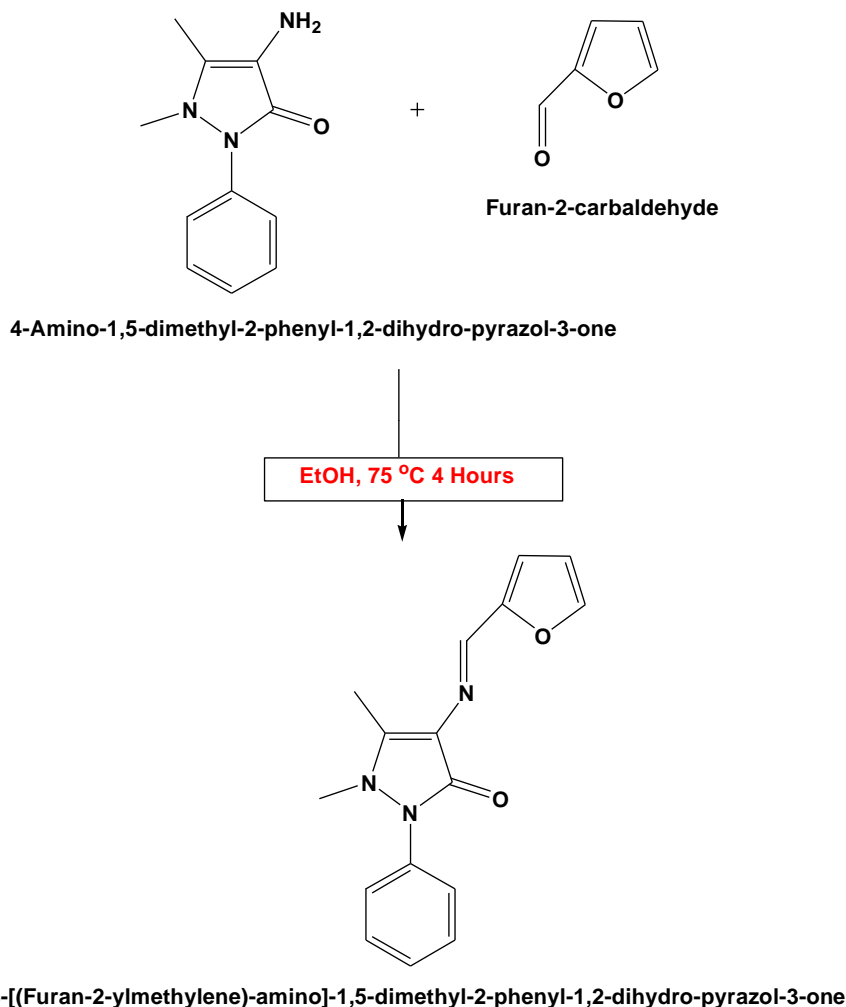
2.1. Chemicals

All chemicals (purity from 98-99%) were purchased and used without further purification. 4-aminoantipyrene, furaldehyde, platinum(IV) chloride, palladium(II) chloride and sodium gold(III) chloride hydrate were received from BDH Company (UK), and other chemicals and solvents used without purification.

2.2. Synthesis of Schiff base ligand

The Schiff base (4APF, Scheme 1) was prepared according to the previous procedure [29-36]: An ethanolic solution of 2-furaldehyde (1 mmol, 25 mL) was added to an ethanolic solution of 4-

aminoantipyrine (1 mmol, 25 mL) and refluxed for 4 hour in a hotplate 75 °C. After cooling of the solution, the precipitate was separated, filtered, re-crystallization with ethanol, and dried over anhydrous calcium chloride under vacuum.



Scheme 1. Preparation design of 4APF Schiff base ligand

2.3. Synthesis of Au(III), Pt(IV) and Pd(II) complexes

To 1.0 mmol solution of PtCl₄ as ((H₂PtCl₆)) (0.410 g), PdCl₂ (0.177) or NaAuCl₄.2H₂O (0.40 g) which dissolved in 20 mL distilled water, the (0.282 g, 1.0 mmol) of 4APF Schiff base ligand dissolved in 40 mL methanol was added and stirred at 70 °C temperature for about 45 min, leading to isolation of solid products which was left overnight till precipitated, washed with methanol and diethyl ether then finally dried under vacuum over anhydrous calcium chloride.

2.4. Measurements

The elemental analyses of carbon, hydrogen and nitrogen contents were performed using a Perkin Elmer CHN 2400 (USA). The molar conductivities of freshly prepared 1.0×10^{-3} mol/cm³

dimethylsulfoxide (DMSO) solutions were measured for the dissolved 4APF complexes using Jenway 4010 conductivity meter. The electronic absorption spectra of 4APF complexes were recorded in DMSO solvent within 900–200 nm range using a UV2 Unicam UV/Vis Spectrophotometer fitted with a quartz cell of 1.0 cm path length. The infrared spectra with KBr discs were recorded on Bruker FT-IR Spectrophotometer (4000–400 cm^{-1}). The Raman laser spectra of the samples were measured on a Bruker FT-Raman spectrophotometer equipped with 50 mW laser. Magnetic data were calculated using Magnetic Susceptibility Balance, Sherwood Scientific, Cambridge Science Park Cambridge, England, at Temp 25°C. The ^1H NMR spectra were recorded on Varian Mercury VX-300 NMR spectrometer. ^1H spectra were run at 300 MHz spectra in deuterated dimethylsulphoxide (DMSO- d_6). Chemical shifts are quoted in δ and were related to that of the solvents. The thermal studies TG/DTG–50H were carried out on a Shimadzu thermogravimetric analyzer under nitrogen till 800 °C. Scanning electron microscopy (SEM) images were taken in Quanta FEG 250 equipment. The X-ray diffraction patterns for the selected nicotinamide complexes were recorded on X'Pert PRO PANalytical X-ray powder diffraction, target copper with secondary monochromate.

2.4. Antibacterial and antifungal activities

Antimicrobial activity of the tested samples was determined using a modified Kirby-Bauer disc diffusion method [44]. Briefly, 100 μL of the best bacteria/fungi were grown in 10 mL of fresh media until they reached a count of approximately 10⁸ cells/mL for bacteria or 10⁵ cells/mL for fungi [45]. 100 μL of microbial suspension was spread onto agar plates corresponding to the broth in which they were maintained. Isolated colonies of each organism that might be playing a pathogenic role should be selected from primary agar plates and tested for susceptibility by disc diffusion method [46, 47]. Of the many media available, National Committee for Clinical Laboratory Standards (NCCLS) recommends Mueller-Hinton agar due to: it results in good batch-to-batch reproducibility. Disc diffusion method for filamentous fungi tested by using approved standard method (M38-A) developed by the NCCLS [48] for evaluating the susceptibility of filamentous fungi to antifungal agents. Disc diffusion method for yeast developed standard method (M44-P) by the NCCLS [49]. Plates inoculated with filamentous fungi as *Aspergillus Flavus* at 25 °C for 48 hours; Gram (+) bacteria as *Staphylococcus Aureus*, *Bacillus subtilis*; Gram (-) bacteria as *Escherichia Coli*, *Pseudomonas aeruginosa* they were incubated at 35–37 °C for 24–48 hours and yeast as *Candida Albicans* incubated at 30 °C for 24–48 hours and, then the diameters of the inhibition zones were measured in millimeters [44]. Standard discs of Tetracycline (Antibacterial agent), Amphotericin B (Antifungal agent) served as positive controls for antimicrobial activity but filter disc impregnated with 10 μL of solvent (distilled water, chloroform, DMSO) were used as a negative control.

The agar used is Mueller-Hinton agar that is rigorously tested for composition and pH. Further the depth of the agar in the plate is a factor to be considered in the disc diffusion method. This method is well documented and standard zones of inhibition have been determined for susceptible values. Blank paper disks (Schleicher & Schuell, Spain) with a diameter of 8.0 mm were impregnated 10 μL of tested concentration of the stock solutions. When a filter paper disc impregnated with a tested chemical

is placed on agar the chemical will diffuse from the disc into the agar. This diffusion will place the chemical in the agar only around the disc. The solubility of the chemical and its molecular size will determine the size of the area of chemical infiltration around the disc. If an organism is placed on the agar it will not grow in the area around the disc if it is susceptible to the chemical. This area of no growth around the disc is known as a "Zone of inhibition" or "Clear zone". For the disc diffusion, the zone diameters were measured with slipping calipers of the National for Clinical Laboratory Standards [46]. Agar-based methods such as Etest disk diffusion can be good alternatives because they are simpler and faster than broth methods [50, 51].

2.5. Anti-Cancer activities

Cytotoxic and antitumor activity of Pd(II), Pt(IV) and Au(III) 4APF synthesized complexes which were tested against MCF-7 cell line according to the method of Mosmann and Vijayan et al., [52, 53]. Inhibitory activity against Breast carcinoma cells (MCF-7 cell line) was detected using different concentration of the tested complexes (A= 50, B= 25, C= 12.5, D= 6.25, E= 3.125 and F= 1.56 μg) and viability cells (%) were determined by colorimetric method.

3. RESULTS AND DISCUSSION

3.1. Physical, micro analytical and molar conductance data

The color, yield (%), conductivity, elemental analysis data and composition of the 4APF complexes are given in table 1.

Table 1. Analytical and physical data for 4APF Schiff base metal complexes

Complexes Empirical formula (M. Wt.)/yield (%)	Color	Λ_m ($\Omega^{-1}\text{cm}^2\text{mol}^{-1}$)	Elemental analysis (%)			
			Found (Calcd.)			
			C	H	N	M
[Pt(4APF)(Cl)].3Cl (618.201)/ 83%	Brown	140	38.98(31.09)	2.42(2.45)	6.64(6.80)	31.21(31.56)
[Pd(4APF)(H ₂ O) ₂].2Cl (494.666)/ 87%	Brown	102	38.44(38.85)	3.63(3.87)	8.16(8.49)	21.28(21.51)
[Au(4APF)(Cl) ₂].Cl (584.635)/ 76%	Brown	60	32.66(32.87)	2.49(2.59)	6.98(7.19)	33.47(33.69)

The experimental of elemental analysis data indicate that all complexes contain 1 nucleus of 4APF moiety. Based on the stoichiometry between metal ion and 4APF ligand, the physical and analytical data (table 1) for the synthesized 4APF complexes is agreement with the proposed molecular formulas: [Pt(4APF)Cl]Cl₃, [Pd(4APF)]Cl₂ and [Au(4APF)(Cl)₂]Cl. The molar conductance values for all complexes (1.0×10^{-3} mol/cm³) were determined in dimethyl sulfoxide (DMSO). The values were $60 \Omega^{-1}\text{cm}^2\text{mol}^{-1}$ for Au(III) complex, $102 \Omega^{-1}\text{cm}^2\text{mol}^{-1}$ for Pd(II) complex and $140 \Omega^{-1}\text{cm}^2\text{mol}^{-1}$ for Pt(IV) complex, these values indicating a slightly electronic nature of Au(III) complex which is due to presence of two chloride ions inside as well as one chloride ion outside the coordination sphere

and electrolyte nature for Pd(II) and Pt(IV) complexes according to the location of chloride ions outside the coordination sphere. The presence of chloride ions inside and outside in all 4APF complexes was detected by addition of few drops of saturated solution of silver nitrate reagent leading to the appearance of white precipitation.

3.2. Mass spectra

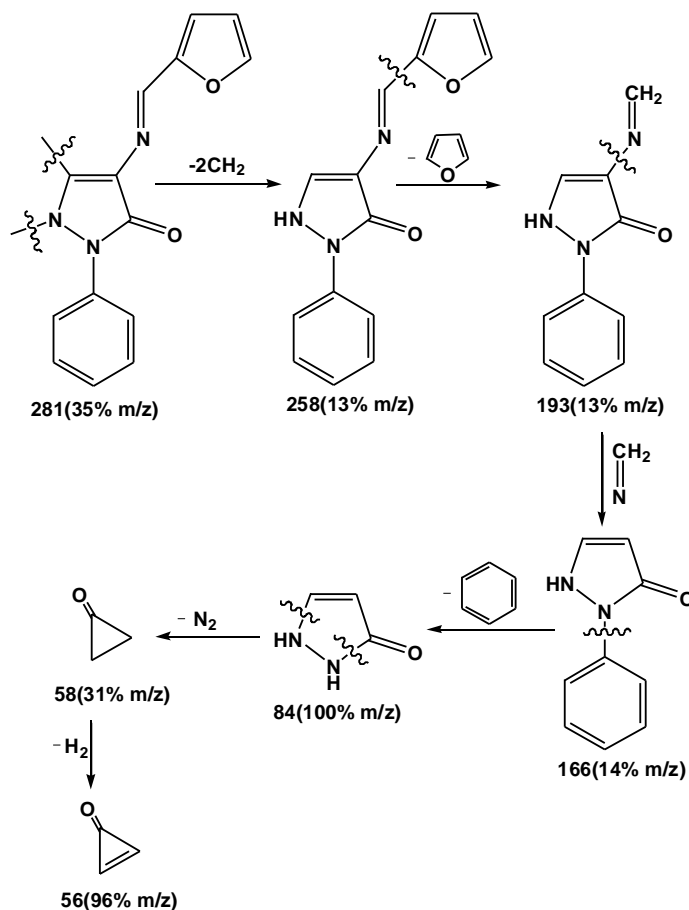


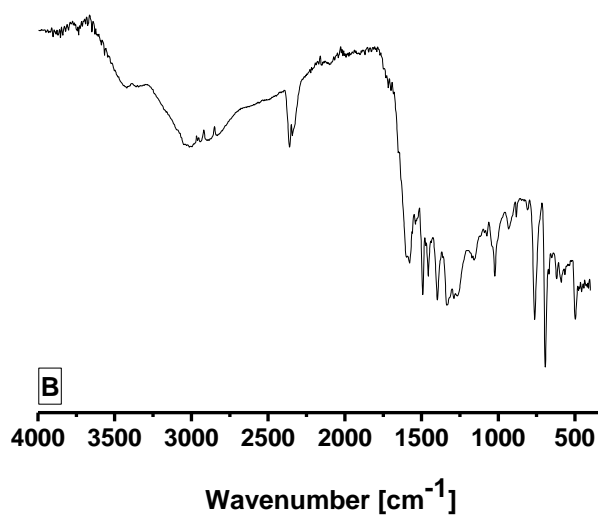
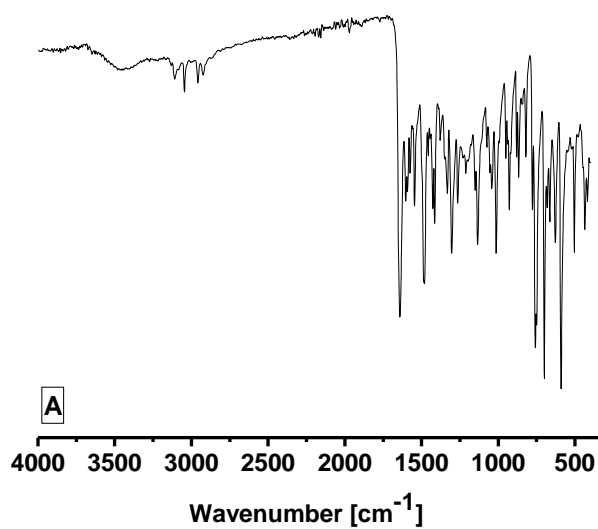
Figure 1. Fragmentation pathway of 4APF Schiff base free ligand

Mass spectroscopic technique has been successfully used to check the molecular ion peaks of free synthetic 4APF Schiff base ligand. The pattern of mass spectrum gives an impression of the successive fragmentations of the Schiff base compound with the series of various peaks corresponding to the different patterns and their intensities. Their intensity gives an idea about stability of fragments. The recorded mass spectrum of the free ligand and molecular ion peaks have been used to confirm the proposed formula (Scheme 1). The mass spectrum of 4APF Schiff base ligand has a prominent base peak 203(100% m/z) shows a peak of the ligand. In 4APF Schiff base ligand, the degradation pattern shows peaks at 281(35% m/z) indicates $[M]^+$ and peaks at 258(13% m/z), 245(18% m/z), 231(36% m/z), 213(13% m/z), 193(13% m/z), 166(14% m/z), 149(14% m/z), 139(38% m/z), 119(60% m/z), 104(17% m/z), 84(100% m/z) and 56(96% m/z), respectively, assigned in (Fig. 1).

3.3. Infrared and Raman spectra

Table 2. IR spectral data of 4APF Schiff base metal complexes

Compounds	Assignments		
	$\nu(\text{C}=\text{O})$	$\nu(\text{CH}=\text{N})$	$\nu(\text{C}-\text{O})$
4APF	1640	1603 1590	1304 1263
[Au(4APF)(Cl) ₂].Cl	1716	1574	1290
[Pt(4APF)(Cl)].3Cl	---	1577	1289
[Pd(4APF)(H ₂ O) ₂].2Cl	1659	1597 1502	1274



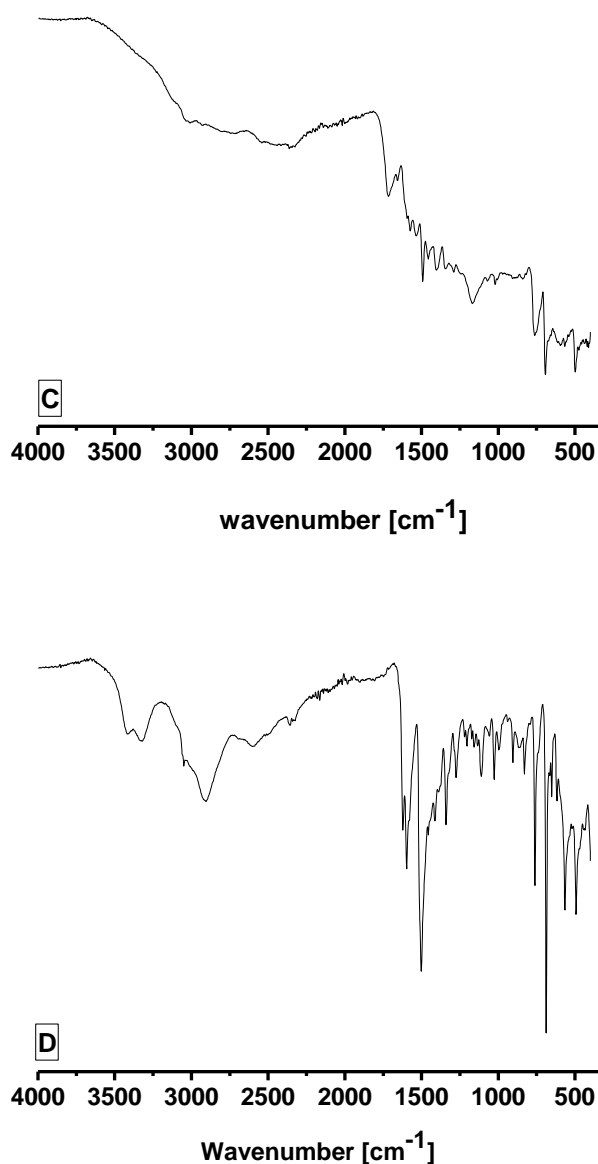


Figure 2. Infrared spectra of (A): 4APF free ligand, (B): Pt^{IV} complex, (C): Au^{III} complex and (D): Pd^{II} complex

Infrared spectra of the three new 4APF Schiff base complexes reveal in comparison with the free ligand displayed with spectral data in table 2 and displayed in Fig. 2. The main infrared spectral data observed the following assignments:

i- the observed band around 1590 cm^{-1} [54] in the free Schiff base ligand is existed at 1577 cm^{-1} , and 1502 cm^{-1} , 1574 cm^{-1} in Pt(IV), Pd(II), and Au(III) complexes, respectively, this band can be attributed to $\nu(\text{C}=\text{N})$ and the shift to lower wavenumber may be understood as a result of involving this group in coordination via nitrogen atom in all 4APF complexes.

ii- The band at 1304 cm^{-1} of the free ligand which may be assigned due to stretching vibration of C-O group [55] in furaldehyde moiety is shifted to lower wavenumber at 1289, 1274 and

1290 cm^{-1} in the spectra of Pt(IV), Pd(II) and Au(III) complexes, respectively, this means that the oxygen of C-O group sharing in the coordination process for all 4APF complexes.

iii- The band around 1640 cm^{-1} with assigned due to stretching vibration band of $\nu(\text{C}=\text{O})$ group in the free ligand spectrum [54, 55] is shifted to higher wavenumbers at 1659 and 1716 cm^{-1} in case of Pd(II) and Au(III) spectra, respectively and this respective band was absent in Pt(IV) complex only, because of unshared in case of Pd(II) and Au(III) 4APF complex but sharing in coordination mode in case of Pt(IV) complex.

iv- A new broad band was observed around 3323 cm^{-1} in Pd(II) complex spectra assigned due to coordinated water molecules [54].

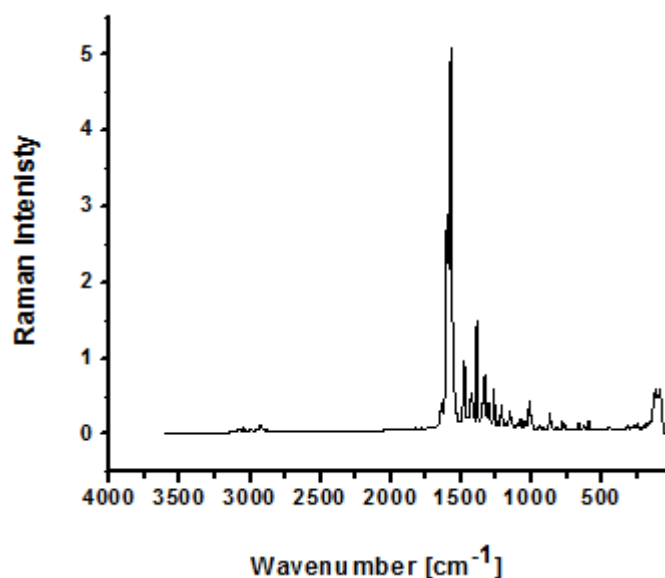


Figure 3a. Raman spectrum of 4APF free ligand

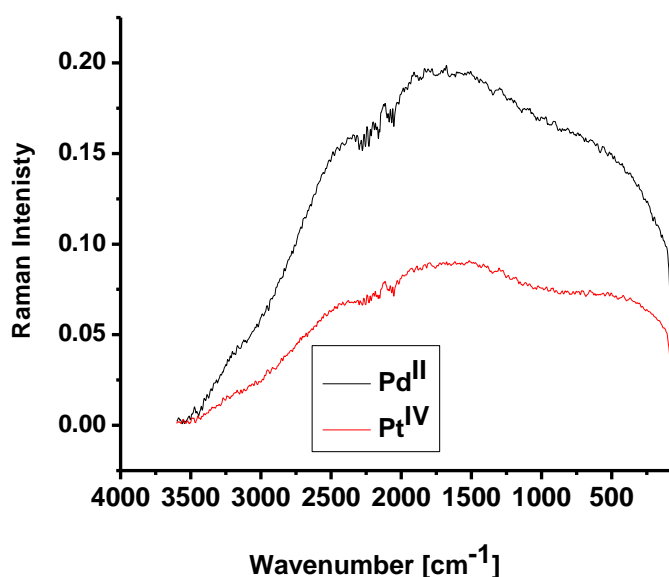


Figure 3b. Raman spectrum of Pd^{II} and Pt^{IV} complexes

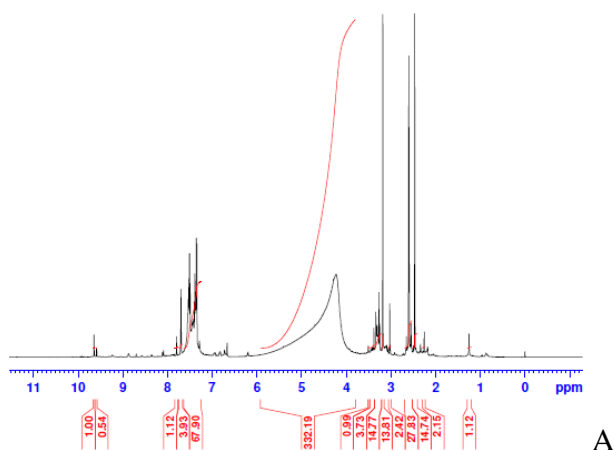
According to the above discussion: Schiff base interact with Pd(II) and Au(III) as a neutral bidentate ligand through the azomethine nitrogen atom and furaldehyde oxygen atom, with two water molecules inside the coordination sphere of the Pd(II) complex and with two chloride ions inside the coordination sphere of Au(III) complex. Schiff base interact with Pt(IV) as a neutral tridentate ligand coordinated via nitrogen of azomethine group, oxygen of furaldehyde moiety and oxygen of carbonyl group with chloride ion inside the coordination sphere and three chloride ions outside the coordination sphere.

Raman spectra of Pt(IV), Pd(II), and Au(III) complexes (Fig. 3) has a scattering and sharp broadening with distorted in the stretching and bending vibration bands, this can be discussed under the knowledge that Raman analysis of fluorescent materials and compounds is a challenging task experimentally due to the overlap of fluorescence which, even when very weak, can overwhelm the inherently weak Raman scattering signal [56, 57].

3.4. UV-vis. electronic spectra

The electronic spectra of the DMSO solutions of the 4APF free ligands, recorded in the 200 – 800 nm exhibit bands in the range 200 – 300 nm and 300 – 400 assigned to the $\pi \rightarrow \pi^*$ and $n \rightarrow \pi^*$ transitions, respectively, of the azomethine group, furaldehyde and 4-aminoantipyrine moieties, and it is shifted to longer wavelength on coordination through azomethine nitrogen in the complexes [57]. The $n \rightarrow \pi^*$ transition undergoes a blue shift indicating that the lone pair electrons of oxygen and nitrogen are coordinated to the metal ion. The $\pi \rightarrow \pi^*$ transition of C=O group of Pt(IV) complex is found at 210 and 225 nm. The $\pi \rightarrow \pi^*$ transition undergoes red shift with an increase in wavelength. Similarly the absorption bands seen at 297 and 388 are attributed to $\pi \rightarrow \pi^*$ and $n \rightarrow \pi^*$ transitions of C = N group. Spectra of all complexes exhibit blue shift for $n \rightarrow \pi^*$ transition which is observed at 387 nm and 384 nm, and a red Shift for the $\pi \rightarrow \pi^*$ (328 nm and 343 nm) transition in all complexes, suggesting the coordination of nitrogen atom. In all complexes charge transition spectra occurred at the 463 nm.

3.5. $^1\text{H-NMR}$ spectra



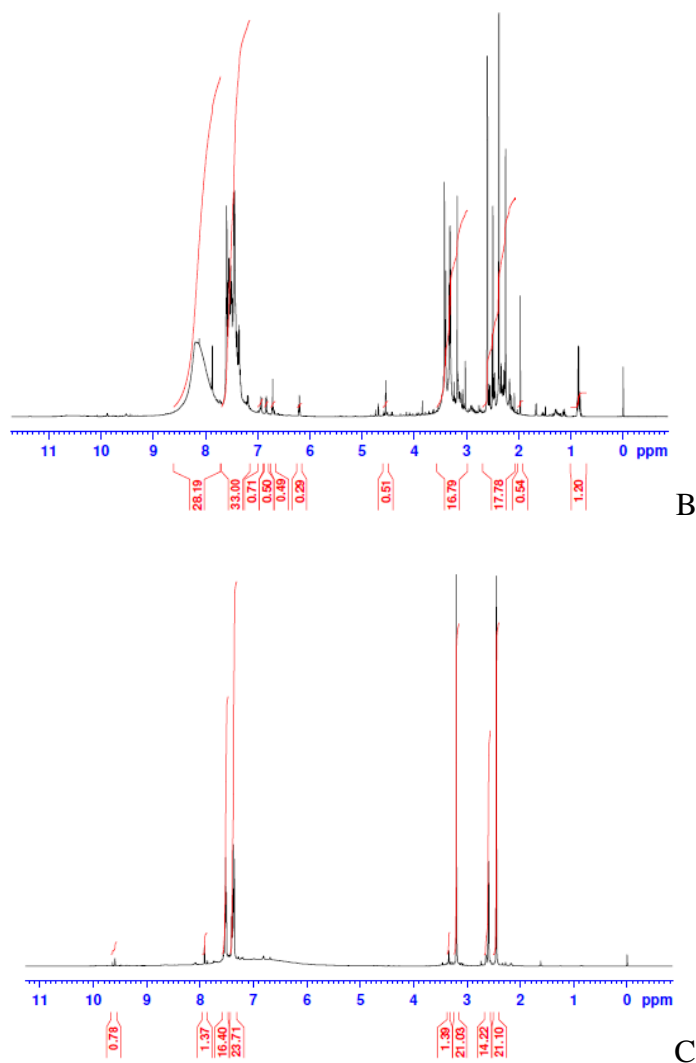


Figure 4. $^1\text{H-NMR}$ spectra of (A): Pt^{IV} complex, (B): Au^{III} complex and (C): Pd^{II} complex

Table 3. $^1\text{H-NMR}$ spectral data of 4APF Schiff base metal complexes

Assignments	Compounds			
	4APF	Au(III)	Pt(IV)	Pd(II)
C- CH_3	2.122	2.255	2.263	2.450
N- CH_3	2.820	2.603	2.614	3.199
Furan ring	6.632 7.299 7.734	6.2-7.3	6.0-7.0	6.0-7.0
HC=N	9.220	8.191	9.723	9.591
Ph; amino antipyrine	7.225 7.422 7.464	7.5-7.8	7.0-8.0	7.0-8.0

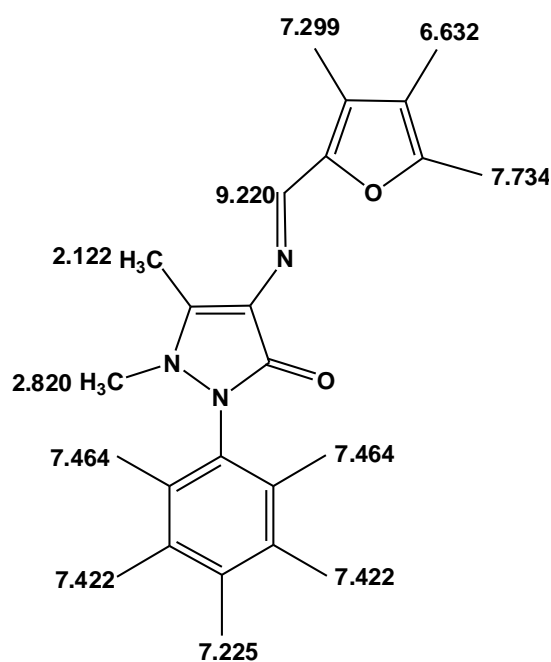
The $^1\text{H-NMR}$ spectra of free 4APF free Schiff base ligand and all $\text{Au}(\text{III})$, $\text{Pt}(\text{IV})$ and $\text{Pd}(\text{II})$ complexes (table 3 and Fig. 4) were recorded to confirm the binding of the Schiff base to the metal ions. $^1\text{H-NMR}$ (300 MHz, $\text{DMSO-}d_6$): δ , 2.122 (3H, C- CH_3 , aminoantipyrine), 2.820 (3H, N- CH_3),

(6.632, 7.299 and 7.734) (3H, furaldehyde), (7.225, 7.422 and 7.464) (5H, Ph, aminoantipyrine) and 9.220 ppm (1H, CH=N).

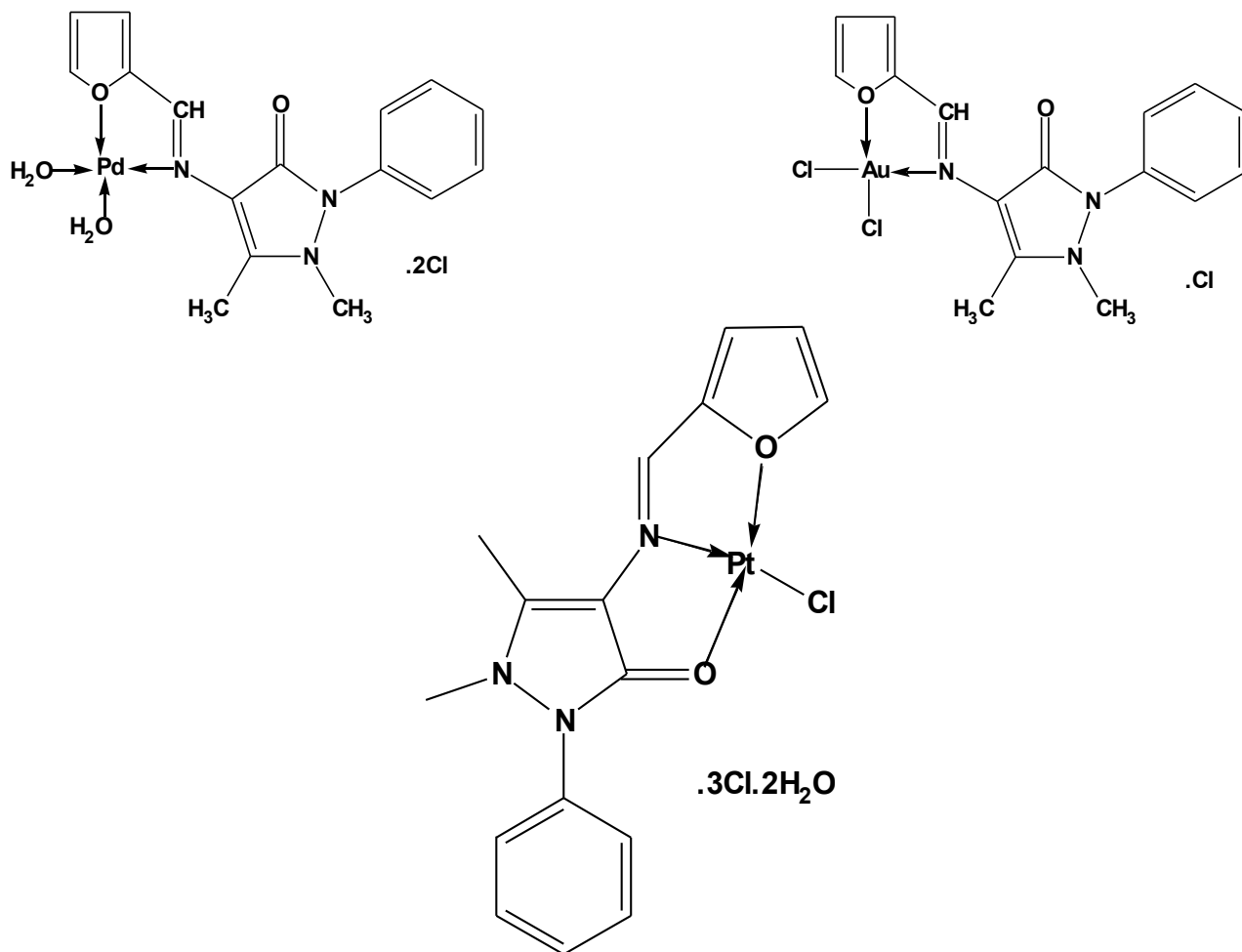
Table 4. Thermal data of the 4APF Schiff base metal complexes

Compounds	Steps	DTG Peak/°C	TG mass loss/%		Assignments
			Calc.	Found	
Pt ^{IV}	1 st	87	2.55	5.809	H ₂ O
	2 nd	207	5.11	5.404	Cl
	3 rd	294	5.11	19.397	3Cl + 4APF (decomposed)
	4 th	457	15.19	38.584	
	Residue				PtO ₂ + residual carbon
Pd ^{II}	1 st	154	15.566	16.678	Phenyl ring
	2 nd	257	22.843	24.197	2H ₂ O + amino antipyrine ring
	3 rd	377	34.000	35.555	Furan ring + Cl ₂
	Residue				PdO + residual carbon
Au ^{III}	1 st	251	34.418	34.843	Amino antipyrine moiety
	2 nd	515	12.144	11.455	2Cl
	3 rd	616	11.472	12.357	Furan moiety
	Residue				Au metal + residual carbon

The spectra of all the complexes showed a singlet peak at δ 9.220 ppm, which has been assigned to the azomethine proton (-HC=N). The position of the azomethine signal in the complexes is shifted in comparison with that of the free ligand, suggesting deshielding of the azomethine proton due to its coordination to metal ions through the azomethine nitrogen.



¹H-NMR data of 4APF free Schiff base ligand



Scheme 2. Suggested structures of 4APF complexes

In the region 7.0 – 8.0 ppm were assigned chemical shifts for hydrogen of symmetrical aromatic ring of ligand. Protons of methyl group attached to carbon or nitrogen atom (C-CH₃- or N-CH₃-) at δ 2.8 or 2.1 ppm, respectively, as singlet peak. The [Pt(4APF)Cl]Cl₃, [Pd(4APF)]Cl₂ and [Au(4APF)(Cl)₂]Cl complexes have the following ¹H-NMR data: δ , 2.263 (3H, C-CH₃), 2.614 (3H, N-CH₃), (6.00, 7.00) (3H, furaldehyde), (7.00, 8.00) (5H, Ph, aminoantipyrine) and 9.723 ppm (1H, CH=N); δ , 2.450 (3H, C-CH₃), 3.199 (3H, N-CH₃), (6.00, 7.00) (3H, furaldehyde), (7.00, 8.00) (5H, Ph, aminoantipyrine) and 9.591 ppm (1H, CH=N); and δ , 2.255 (3H, C-CH₃), 2.603 (3H, N-CH₃), (6.20, 7.30) (3H, furaldehyde), (7.00, 8.00) (5H, Ph, aminoantipyrine) and 8.191 ppm (1H, CH=N), respectively. On the basis of the above studies; the suggested structures of the 4APF complexes can be represented in Scheme 2.

3.6. SEM, EDX and XRD spectra

The x-ray powder diffraction patterns for the new 4APF Schiff base complexes, [Pt(4APF)Cl]Cl₃, [Pd(4APF)]Cl₂ and [Au(4APF)(Cl)₂]Cl are depicted in Fig. 5.

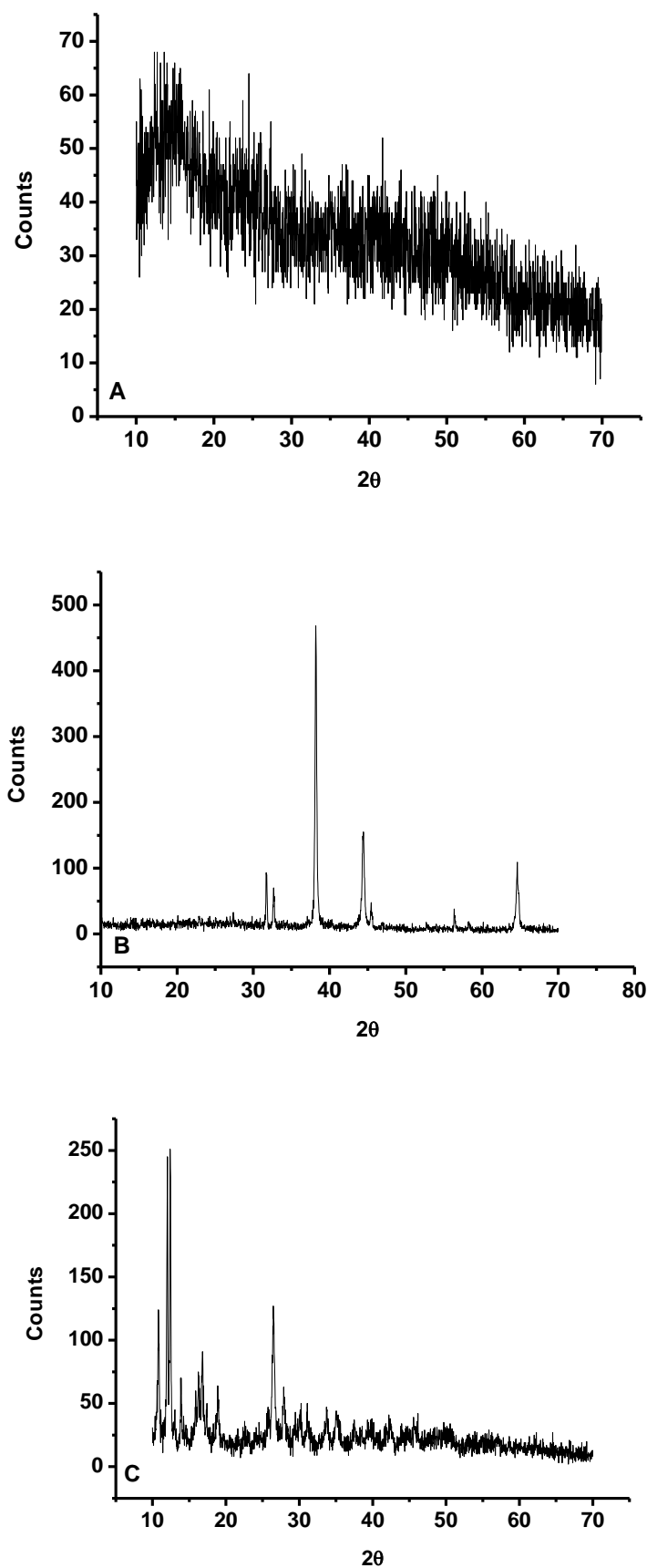


Figure 5. XRD spectra of (A): Pt^{IV} complex, (B): Au^{III} complex and (C): Pd^{II} complex

Inspecting these patterns, we notice that the systems [Au(4APF)(Cl)₂]Cl, [Pd(4APF)]Cl₂ and [Pt(4APF)Cl]Cl₃ are well crystalline, semi-crystalline and amorphous, respectively. The definite diffraction data like angle (2θ), interplanar spacing (d value, Angstrom), and relative intensity (%) have been calculated. The values of 2θ, d value (the volume average of the crystal dimension normal to diffracting plane), full width at half maximum (FWHM) of prominent intensity peak, relative intensity (%) and particle size of gold(III) and palladium(II) complexes were estimated. The maximum diffraction patterns of Au^{III} and Pd^{II} complexes exhibited at 2θ (Intensity (counts)) = 38(100%) and 12(100%), respectively. The crystallite size could be estimated from XRD patterns by applying FWHM of the characteristic peaks using Deby-Scherrer equation 1 [58].

$$D = K\lambda/\beta\cos\theta \dots\dots\dots (\text{equ. 1})$$

Where D is the particle size of the crystal grain, K is a constant (0.94 for Cu grid), λ is the x-ray wavelength (1.5406 Å), θ is the Bragg diffraction angle and β is the integral peak width. The particle size was estimated according to the highest value of intensity compared with the other peaks. These data gave an impression that the particle size of gold(III) complex located within nano scale range. Surface image using SEM (Fig. 6) demonstrate to the structures of surface of prepared Schiff base complexes.

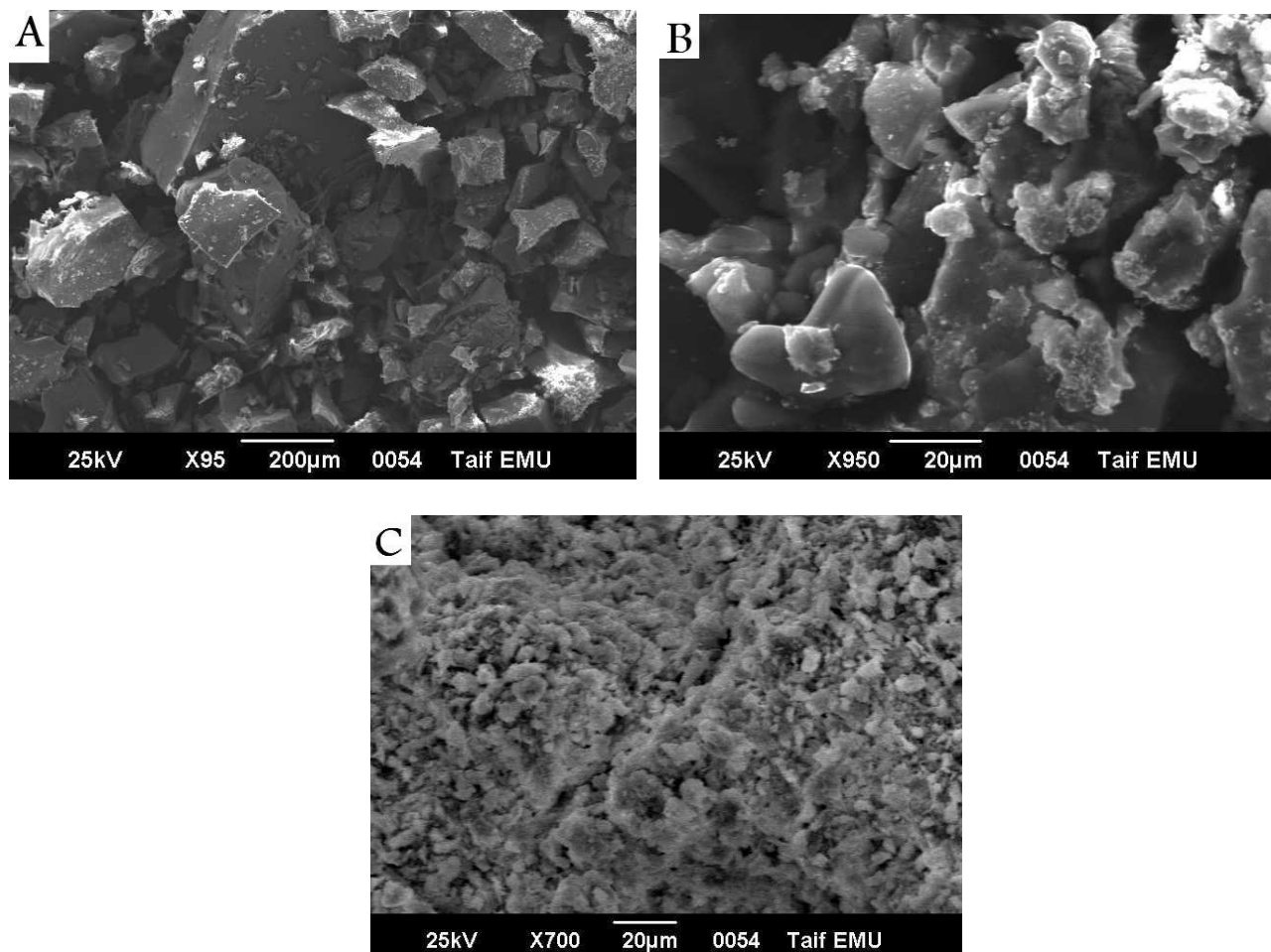
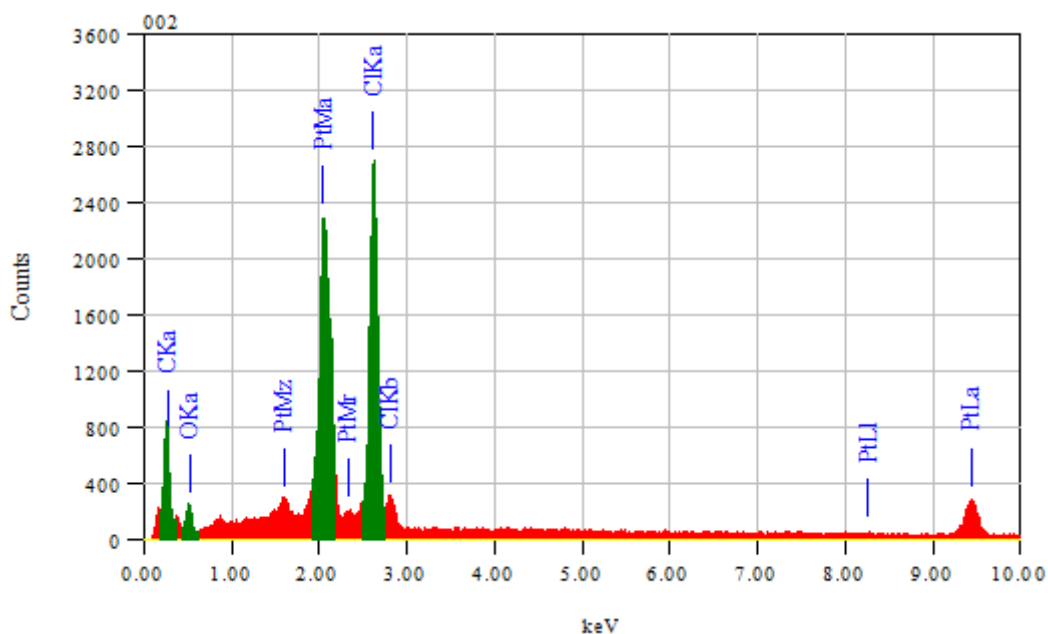
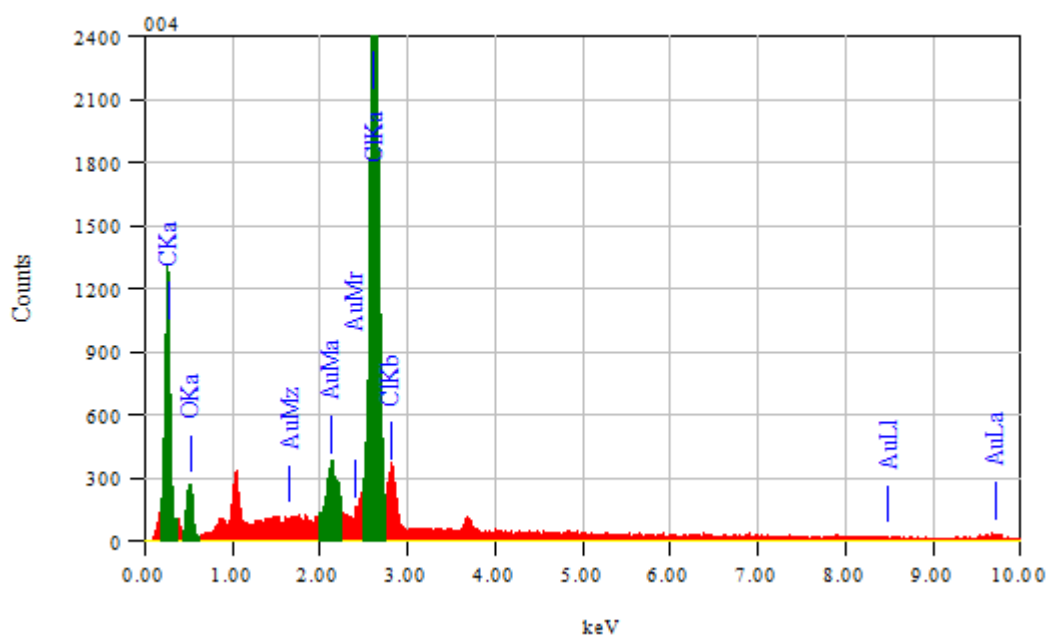


Figure 6. SEM pictures of (A): Pt^{IV} complex, (B): Au^{III} complex and (C): Pd^{II} complex

Analysis of these images shows the size of pores to be quite different with different metal ions. The chemical analysis results by EDX for the formed Schiff base complexes show a homogenous distribution of each metal ion. SEM examinations were checked the surfaces of these Schiff base complexes that show a small to medium particles which tendency to agglomerates formation with different shapes comparison with the start materials. The chemical compositions of the Schiff base complexes were determined using energy-dispersive X-ray diffraction (EDX). In the EDX profile of these complexes (Fig. 7), the peaks of the essential two elements like carbon and oxygen, and respective gold(III), palladium(II) and platinum(IV) elements, which constitute the molecules of $[\text{Au}(4\text{APF})(\text{Cl})_2]\text{Cl}$, $[\text{Pd}(4\text{APF})]\text{Cl}_2$ and $[\text{Pt}(4\text{APF})\text{Cl}]\text{Cl}_3$ complexes, are clearly identified confirming the proposed structures.



A



B

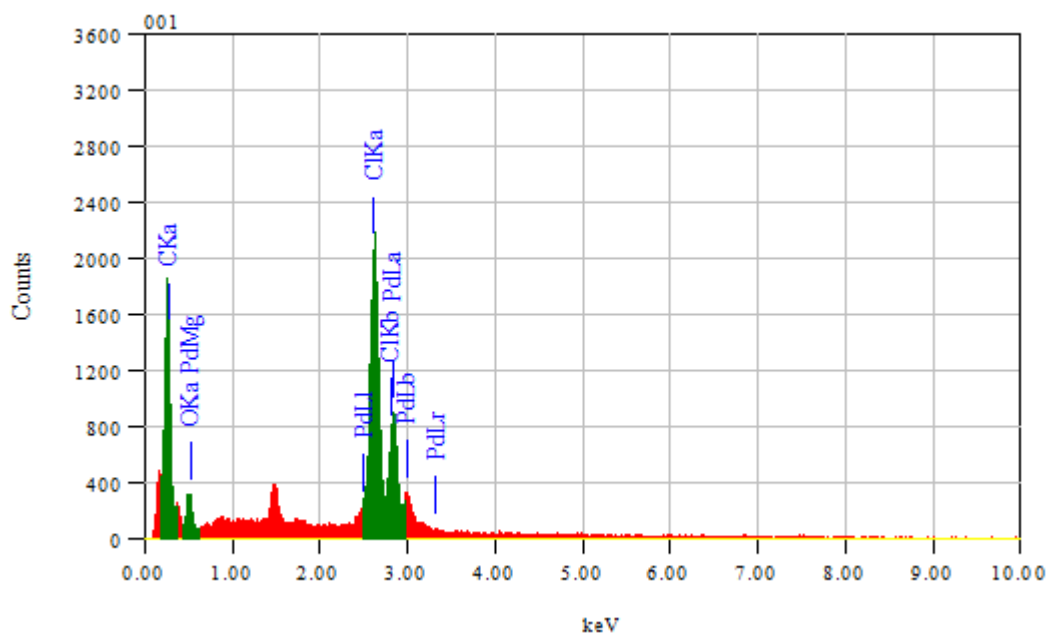


Figure 7. EDX analyses of (A): Pt^{IV} complex, (B): Au^{III} complex and (C): Pd^{II} complex

3.7. Thermo gravimetric analysis

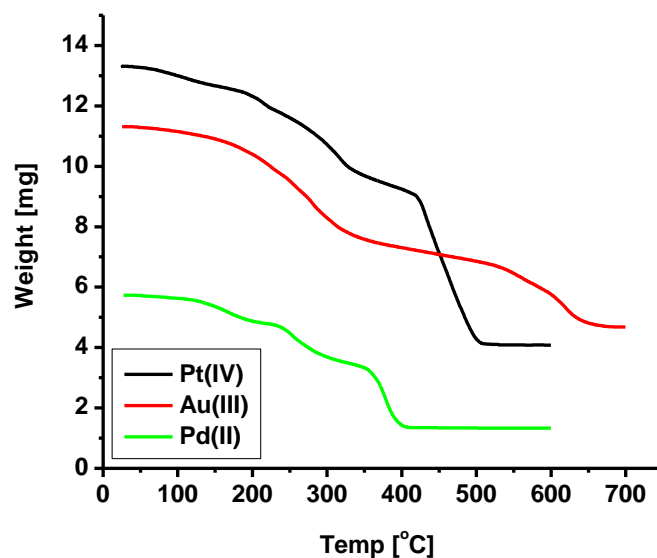


Figure 8. TG curves of Pt^{IV}, Au^{III} and Pd^{II} complexes

Figure 8 and table 4 give the maximum temperature values for the decomposition along with the species lost in each step of the decomposition reactions of the 4APF [Au(4APF)(Cl)₂]Cl, [Pd(4APF)]Cl₂ and [Pt(4APF)Cl]Cl₃ complexes. The decomposition occurs in at least three major detectable steps, each step does not referred in generally to single process but rather is reflects of two or three overlapping process and attributed to the ligand alone or accompanied by chlorine atoms. The data obtained support the proposed structure and indicate that Pt(IV) complex undergo four steps

degradation reaction, the first step occur at maximum peak lying in 87 °C, the weight loss associated with this step agrees quite well with the loss two uncoordinated water molecules, the second step occur at T_{max} 207 °C, and it referred to loss one of chlorine atom, and the third and fourth decomposition steps not referred to a single process but its reflective of two or three overlapping processes and attributed to loss of the 4-amino antipyrine, three chlorine atoms and furan moieties. The residual is in agreement with PtO_2 polluted with few carbon atoms. The thermal decomposition of Au(III) complex may be characterized as a three decomposition steps in temperature range 125-392 °C, the first stage 125-191 °C ($T_{max} = 145$ °C) is due to initial decomposition of this complex and occurs in an overlapping reaction with mass lose 34.843% for 4-amino antipyrine, concerning second and third decomposition steps at 532-574 °C ($T_{max}= 515$ °C) with mass loss of 11.455%, and 601-641 °C ($T_{max}= 616$ °C) with mass loss of 12.357% assigned to liberated two chlorine atoms and furan moiety. The residual is in agreement with gold metal attached with four carbon atoms. For the pd(II) complex the first mass loss is due to losses phenyl group and occurs between 125 °C and 191 °C, and has loss of 16.678% which means the decomposition of antipyrine nucleus stat in this stage, then, the rest of antipyrine decomposed in the second stage between 239 and 278 °C with mass loss 24.197%, the last stage occurred between 361 °C and 392 °C and is due to release furan moiety and both chlorine atoms with mass loss about 35.555%. The residual is in agreement with PdO.

3.8. Anti-microbial assessments

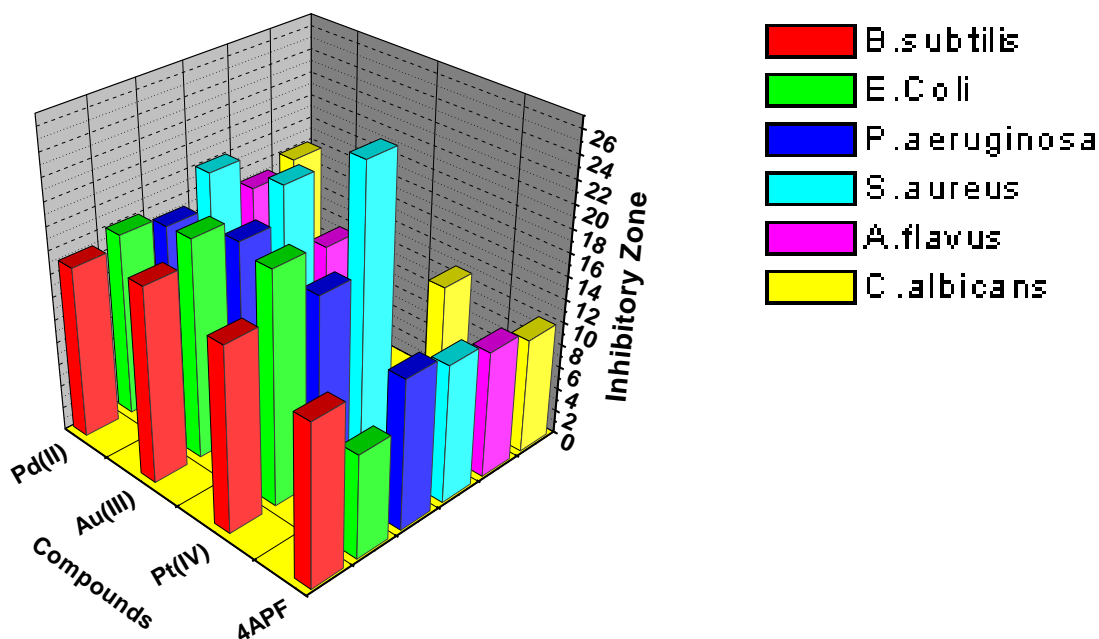


Figure 9. Inhibitory zone of 4APF Schiff base and their complexes against some kind of bacteria (+/-) and fungi

The 4APF Schiff base ligand and their metal complexes were evaluated for their antibacterial activity against bacterial species *Escherichia coli* (a), *Staphylococcus aureus* (b) and *Pseudomonas aeruginosa* (c) as well as antifungal activity against species (d) *Aspergillus Flavus* and (e) *Candida Albicans*. The compounds were tested at a concentration of 30 $\mu\text{g}/0.01\text{ mL}$ in DMF solution using the paper disc diffusion method. The susceptibility zones were measured in diameter (mm) and the results are reproduced in Fig. 9. The susceptibility zones measured were the clear zones around the discs killing the bacteria and fungi. All the Schiff bases and their complexes individually exhibited varying degrees of inhibitory effects on the growth of the tested bacterial species. The antibacterial results evidently show that the activity of the Schiff base ligand became more pronounced when coordinated to the metal ions [59, 60]. It is suggested that in the chelated complex, the positive charge of the metal is partially shared with the donor atoms present in the ligands and there is electron delocalization over the whole chelate ring. This in turn increases the lipophilic character of the metal chelate and favors its permeation through the lipid layers of the bacterial membranes. Apart from this, other factors such as solubility, conductivity and dipole moment (influenced by the presence of metal ions) may also be the possible reasons for increasing this activity.

3.9. Antitumor Activity

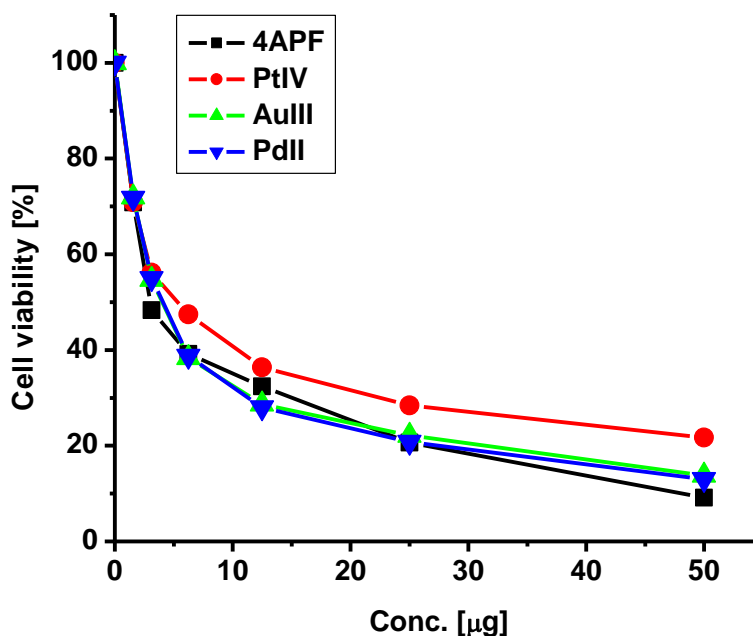


Figure 10. Antitumor test of 4APF Schiff base and their Pt(IV), Au(III) and Pd(II) complexes

From the cytotoxicity profiles, Fig. 10, it could be concluded that the Pt(IV), Au(III) and Pd(II) complexes have a significant antitumor activity against breast carcinoma cells (MCF-7 cell line). The half maximum inhibitory concentrations (IC_{50}) of all complexes against breast carcinoma cells were detected by using different concentration of the tested compounds (50, 25, 12.5, 6.25, 3.125 and 1.56 μg) and viability cells (%) were determined by colorimetric method. Also, inhibitory concentration

fifty (IC_{50}) was displayed in Fig. 10. Inhibitory concentration fifty (IC_{50}) was found to be 3.2 μg for free 4APF Schiff base ligand, 4.7 μg for Pt(IV) complex, 3.82 μg for Au(III) complex, 6.18 μg for Pd(II) complex. This paper indicates that clinically achievable concentrations of 4APF Schiff base may be useful against breast carcinoma cells (MCF-7 cell line). Finally, it is concluded that a significant antitumor activity of Pt(IV), Au(III) and Pd(II) complexes against breast carcinoma cell lines could be explained as cellular damage. The mechanism of action of these complexes involves binding to DNA and RNA of carcinoma cell by the ability of the nucleobases and nucleotides to be subject to attack on Pt(IV), Au(III) and Pd(II). This action agrees with this result which indicated that the antitumor activity of tested complexes increase with its concentrations [61, 62]. These findings prompt to search for possible interaction of these complexes with other cellular elements and further studied required to investigate the possible side effect of tested complexes on normal living cell.

References

1. T. Radhakrishnana, P.T. Joseph, C.P. Prabhakaran, *J. Inorg.Nucl. Chem.*, 38 (1976) 2212.
2. G. Shankar, R.P. Premkumar, S.K. Ramalingam, *Polyhedron*, 5 (1986) 991.
3. J.J. Li, Pyrazole Synthesis, Springer, Berlin Heidelberg, New York, 2006, pp. 331-334.
4. P.M.P. Santos, A.M.M. Antunes, J. Noronha, E. Fernandes, A.J.S.C. Vieira, *Eur.J. Med. Chem.*, 45 (2010) 2258.
5. T. Rosu, E. Pahontu, C. Maxim, R. Georgescu, N. Stanica, A. Gulea, *Polyhedron*, 30 (2011) 154.
6. E. Radzikowska, K. Onish, E. Chojak, *Eur. J. Cancer*, 31 (1995) 5225.
7. K.L. Khanduja, S.C. Dogra, S. Kavshal, R.R. Sharma, *Biochem. Pharmacol.*, 33 (1984) 449.
8. I.D. Capel, M. Jenner, M.H. Pinnock, D.C. Williams, *Biochem. Pharmacol.*, 27 (1978) 1413.
9. G. Plesch, M. Blahova, J. Kratsmarsmogrovic, C. Friebel, *Inorg. Chim. Acta*, 136 (1987) 117.
10. S. Cunha, S.M. Oliveira, M. Rodrigues Jr., R.M. Bastos, J. Eerrari, H.B. Napolitano, I. Vencato, C. Lariucci, *J. Mol. Struct.*, 752 (2005) 32.
11. S. Bondock, R. Rabie, H.A. Etman, A.A. Fadda, *Eur. J. Med. Chem.*, 43 (2008) 2122.
12. M.A. Madiha, A. Rania, H. Moataz, S. Samira, B. Sanaa, *Eur. J. Pharmacol.*, 569 (2007) 222.
13. A.N. Evstropov, V.E. Yavorovskaya, E.S. Vorob'ev, Z.P. Khudonogova, S.G. Medvedeva, V.D. Filimonov, T.P. Prishchep, A.S. Saratikov, *Pharm. Chem. J.*, 26(5) (1992) 426.
14. S.E. Forest, M.J. Stimson, J.D. Simon, *J. Phys. Chem. B*, 103 (1999) 3963.
15. G. Turan-Zitauni, M. Sivaci, F.S. Kilic, K. Erol, *Eur. J. Med. Chem.*, 36 (2001) 685.
16. M.S. Collado, V.E. Manotorani, H.C. Goicoechea, A.C. Olivieri, *Talanta*, 52 (2000) 909.
17. S.A. Coolen, T. Ligor, V. Lieshout, F.A. Huf, *J Chromatogr. B Biomed. Sci. Appl.*, 732 (1999) 103.
18. D. Sinha, A.K. Tiwari, S. Singh, G. Shukla, P. Mishra, H. Chandra, A.K. Mishra, *Eur. J. Med. Chem.*, 43 (2008) 160.
19. B.S. Torrog, D.J. Kitko, R.S. Drag, *J. Am. Chem. Soc.*, 98 (1976) 5144.
20. K.C. Emregul, E. Duzgun, O. Atakol, *Corros. Sci.*, 48 (2006) 3243.
21. R. Drozdak, B. Auaert, N. Ledoux, I. Dragutan, V. Dragutan, F. Verpoort, *Coord. Chem. Rev.*, 249 (2005) 3055.
22. J.L. Seeler, P.J. Melfi, G. Dan Pantes, *Coord. Chem. Rev.*, 250 (2006) 816.
23. G.G. Hammes, P. Fasella, *J. Amer. Chem. Soc.*, 84 (1962) 4644.
24. I.M.I. Fakhir, N.A. Hamdy, N.A. Hamdy, M.A. Radwan, Y.M. Ahmed, *Egypt J. Chem.*, (2004) 201.
25. P.S. Dixit, K. Srinivasan, *Inorg. Chem.*, 27 (1988).
26. A.M. Mahindra, *J.M. Fisher*, 303 (1983) 64.
27. P.R. Palet, B.T. Thaker, S. Zele, *Indian J. Chem.*, A38 (1999) 563.
28. R.E. Hester, E.M. Nour, *J. Raman Spectrosc.*, 11 (1981) 49.
29. A.F. Kolodziej, *Prog. Inorg. Chem.*, 41 (1994) 493.

30. N. Raman, J.D. Rajia, A. Sokthivel, *J. Chem. Sci.*, 119 (2007) 303.
31. P.M. Selvakumar, E. Suresh, P.S. Subramania, *Polyhedron*, 26 (2007) 749.
32. P.K. Agarwal, L. Singh, D. Sharma, L. Singh, H. Agarwal, *Bioinorg. Chem. Appl.*, (2006). Doi: 1155/BCA/2006/29234 Article ID 24 234.
33. N. Raman, A. Kulandaisamy, *Trans. Met. Chem.*, 29 (2004) 129.
34. K.Z. Ismail, *Trans. Met. Chem.*, 25 (2000) 522.
35. A. El-issouky, A.K. Shehata, G. El-Mahdey, *Polyhedron*, 16 (1997) 1247.
36. T. Rosa, S. Pasculescu, V. Lazar, C. Chifiriuc, *Molecules*, 11 (2006) 904.
37. T. Rosu, M. Negoiu, S. Pasculescu, E. Pahontu, D. Poirier, A. Gulea, *Eur. J. Med. Chem.*, 45 (2010) 774.
38. Y. Sun, Q. Hao, W. Wei, Z. Yu, L. Lu, X. Wang, Y. Wang, *J. Mol. Struct.*, 929 (2009) 10.
39. V.C. Filho, R. Correa, Z. Vaz, T.B. Calixto, R.J. Nunes, T.R. Pinheino, A.D. Andicopulo, R.A. Yunes, *Farmaco*, 53 (1998) 55.
40. S.M. Sondhi, V.K. Sharma, R.P. Verma, N. Singhal, R. Shukla, R. Raghubir, M.P. Dubey, *Synthesis* (1999) 878.
41. A.P. Mishra, *J. Indian Chem. Soc.*, 76 (1999) 35.
42. N. Raman, A. kulaudaisawy, K. Jegasubramanian, *Syn. React. Inorg. Metal-Org. Chem.*, 34 (2004) 7.
43. A.W. Bauer, W.M. Kirby, C. Sherris, M. Turck, *Amer. J. Clinical Pathology*, 45 (1966) 493.
44. M.A. Pfaller, L. Burmeister, M.A. Bartlett, M.G. Rinaldi, *J. Clin. Microbiol.* 26 (1988) 1437.
45. National Committee for Clinical Laboratory Standards, Performance Vol. antimicrobial susceptibility of Flavobacteria, 1997.
46. National Committee for Clinical Laboratory Standards. 1993. Methods for dilution antimicrobial susceptibility tests for bacteria that grow aerobically. Approved standard M7-A3. National Committee for Clinical Laboratory Standards, Villanova, Pa.
47. National Committee for Clinical Laboratory Standards. (2002). Reference Method for Broth Dilution Antifungal Susceptibility Testing of Conidium-Forming Filamentous Fungi: Proposed Standard M38-A. NCCLS, Wayne, PA, USA.
48. National Committee for Clinical Laboratory Standards. (2003). Methods for Antifungal Disk Diffusion Susceptibility Testing of Yeast: Proposed Guideline M44-P. NCCLS, Wayne, PA, USA.
49. L.D. Liebowitz, H.R. Ashbee, E.G.V. Evans, Y. Chong, N. Mallatova, M. Zaidi, D. Gibbs, and Global Antifungal Surveillance Group. 2001. *Diagn. Microbiol. Infect. Dis.* 4, 27.
50. M.J. Matar, L. Ostrosky-Zeichner, V.L. Paetznick, J.R. Rodriguez, E. Chen, J.H. Rex, *Antimicrob. Agents Chemother.*, 47 (2003) 1647.
51. T. Mosmann, *J. immunol. Methods*, 65 (1983) 55.
52. P. Vijayan, C. Ragha, G. Ashok, S.A. Doanraj, B. suresh, *Indian J. Med. Res.*, 120 (2004) 24.
53. L.J. Bellamy, "The Infrared Spectra of Complex Molecules, 3rd Ed., Chapman and Hall, London, 1975.
54. K. Nakamoto, "Infrared and Raman Spectra of Inorganic and Coordination Compound", Wiley, New York, 1978.
55. S.E.J. Bell, N.M.S. Sirimuthu, *Chem. Soc. Rev.* 37 (2008) 1012.
56. M.R. Kagan, R.L. McCreery, *Anal. Chem.* 66 (1994) 4159.
57. H.H. Jaffe, M. Orehin. Theory and application of ultraviolet spectroscopy, John Willey and sons, New York, 1982.
58. C.X. Quan, L.H. Bin, G.G. Bang, *Mater. Chem. Phys.* 91 (2005) 317.
59. S.K. Bharti, G. Nath, R. Tilak, S.K. Singh, *Eur. J. Med. Chem.* 45(2) (2010) 651.
60. Z.H. Chohan, S.H. Sumrra, M.H. Youssoufi, T.B. Hadda, *Eur. J. Med. Chem.* 45(7) (2010) 2739.
61. X.U. Dongfang, M.A. Shuzhi, D.U. Guangying, H.E. Qizhuang, S. Dazhi, *J. Rare Earths* 26(5) (2008) 643.

62. N. Zhang, Yu-hua Fan, Z. Zhang, J. Zuo, Peng-fei Zhang, Q. Wang, Shan-bin Liu, Cai-feng Bi,
Inorg. Chem. Comm. 22 (2012) 68.

© 2013 by ESG (www.electrochemsci.org)